NANOINDENTATION OF SMECTITE- AND SERPENTINE-RICH CARBONACEOUS CHONDRITES

Christian G. Hoover[1], Laurence A.J. Garvie[2,3] , Desiree Cotto-Figueroa[4] and Erik Asphaug[5] [1]School of Sustainable Engineering and the Built Environment, Ira A. Fulton Schools of Engineering, ASU, Tempe AZ 85287 (christian.hoover@asu.edu), [2]Buseck Center for Meteorite Studies, [3]School of Earth and Space Exploration, ASU, AZ 85287-6004. [4]Department of Physics and Electronics, University of Puerto Rico at Humacao, Call Box 860, Humacao, PR 00792, Puerto Rico [5]Lunar and Planetary Laboratory, UofA, Tucson, AZ 85721.

Introduction: Clay-rich rocks can have complex material compositions controlled by the abundant porous embedding clay matrix material and stiffer inclusions, which could range in size from < 1 μm to several hundred μm. Similarly, many carbonaceous chondrites (CC), of petrologic type 1 and 2, are argillaceous rocks and dominated by phyllosilicates and other clays-sized minerals [1]. Bulk powder XRD shows that the clays are dominated by serpentines and smectites [2]. This multiscale heterogeneity gives rise to different mechanical behaviors on different scales. On smaller scales, it is possible to probe the mechanics of a single material phase through highly localized tests, whereas on larger scales, any response will be a combination of the effects across multiple material phases on smaller scales for example in measurements such as sound speed tests, which can be used on millimeter scales to determine bulk material properties [3]. The behaviors of individual anhydrous phases and the clay matrix is less understood, though interest is growing for such tests for returned samples like Ryugu [4]. Here, we use instrumented nanoindentation to determine the properties of the clay matrix, which can be elucidated thanks to phase separability [5].

Samples and Testing Protocol: Two clay-rich carbonaceous chondrites were prepared as polished epoxy mounts (i) Tarda (C2-ung), whose clay matrix is made of smectite, serpentine, and interstratified serpentine/smectite with embedded magnetite [6], and (ii) Aguas Zarcas (CM2), whose matrix is dominated by serpentine with variable ferrotochilinite and interstratified ferrotochilinite/cronstedtite [7]. All samples were dry-polished and free of epoxy. Data was recorded using a Ultra Nano Hardness Tester[3] (UNHT[3]) from Anton Paar. Indents made with a 3-sided pyramid Berkovic indenter and were loaded in force-control up to their limiting maximum force of 1.8 mN. The load-hold-unload time for each test was 10-5-10 seconds, following an established protocol used on organic-rich rocks [8]. The spatial distance between each indent was 10 μm. The raw data output is a load versus load point displacement curve at every indent. The modulus (*M*) and hardness (*H*) of the material(s) are found using the Oliver and Pharr model [9,10].

Results and Discussion: Two grids were performed on Aguas Zarcas consisting of 150 indents in each (Fig. 1,a-d) and one grid was performed on Tarda with 400 indents (Fig. 1,e-f). Since indentation is essentially a surface test, it is unknown if a single indent will probe a single material phase, as there could be other phases beneath the surface that contribute to the mechanical response. This, and the spatially variable porosity in the clay matrix, gives rise to some uncertainty in the mechanical properties, shown in scatter plots of *M* versus *H* (Fig. 1, a,c&e). Analysis of the indentation results requires the use of statistical tools to categorize different material-based mechanical phases present within the probed region. Here, we use a multi-variate cluster algorithm [11] to provide the most likely number of statistical clusters in a data set, as well as the uncertainty of observations belonging to a cluster based on statistical criteria. The clustering algorithm partitioned the data for each grid into statistical phases, the mean indentation curve belonging to each phase was plotted in (Fig. 1, b,d&f).

Tarda shows four distinct phases, whereas Aguas Zarcas Grid (i) is has two and Grid (ii) has three phases. The mean and standard deviation for *M*, *H* and *M/H*, which is an indicator of ductility, as well as the volume fraction of points belonging to each phase are listed in Table 1. The *M* for phase 1 of Tarda falls within the range of montmorillonite, and has a *M* between 7.3 - 72.3 [12] for the x3 and x1 directions respectively, and for a collection of particles with randomly oriented directions, 33-39.5 [13], indicating that the points belonging to Phase 1 are dominated by the mechanics of smectite. This differs greatly from the serpentine-rich clay matrix of the Aguas Zarcas, which was found to have a modulus much less than Tarda. The other phases contain influences from stiffer inclusions, which have higher moduli than the clays.

Conclusions: The CCs studied here show considerable differences in their mechanical response. The more compliant phase response curves that penetrate deeper into the matrix, suggesting that that the mechanical response on larger scales could be governed by these phases. The data shown by the CCs are also of interest because similar materials are thought to be present on asteroids 101955 Bennu and Ryugu. Thus, the detailed study of the CCs provides the framework and basic knowledge with which to study the samples returned from hydrated, clay-rich asteroids.

Acknowledgement: All samples are from the Buseck Center for Meteorite Studies at ASU. The authors are grateful for the support for this research, provided by the NASA YORPD program through grant 80NSSC22K023.

References: [1] Kuila and Prasad (2013) Geophys Prospecting, 61, 341-362. [2] Brearley and Jones (1998) Rev. Mineral., 36, 3-1 – 3-398. [3] Flynn G.J. et al. (2018) *Chem. Erde*, 78, 269-298. [4] Nakamura T. et al. (2022) *Science*, 10.1126/science.abn8671. [5] Ulm F. J. et al. (2010) *Cem. Concr. Compos., 32*, 92–99. [6] Garvie L. A. J. and Trif L. (2021) *52nd LPSC,* Contribution No. 2548. [7] Garvie L. A. J. (2021) *Am. Min*., 106, 1900-1916. [8] Abedi S. et al. (2016) *Acta Geotech*, 11, 559-572. [9] Oliver W.C. and Pharr G.M. (2004) *J. Mater. Res.,* 19, 3-20. [10] Oliver W.C. and Pharr G.M. (1992) *J. Mater. Res.,* 7, 1564-1583. [11] Fraley C. and Raftery A. E. (1999) *J. Classif.*, 16(2):297–306. [12] Berthonneau J. et al. (2017) *Appl. Clay Sci*, 143, 387-398. [13] Mondol N. H., et al. (2008) *Lead. Edge*, 27 (6): 758–770.

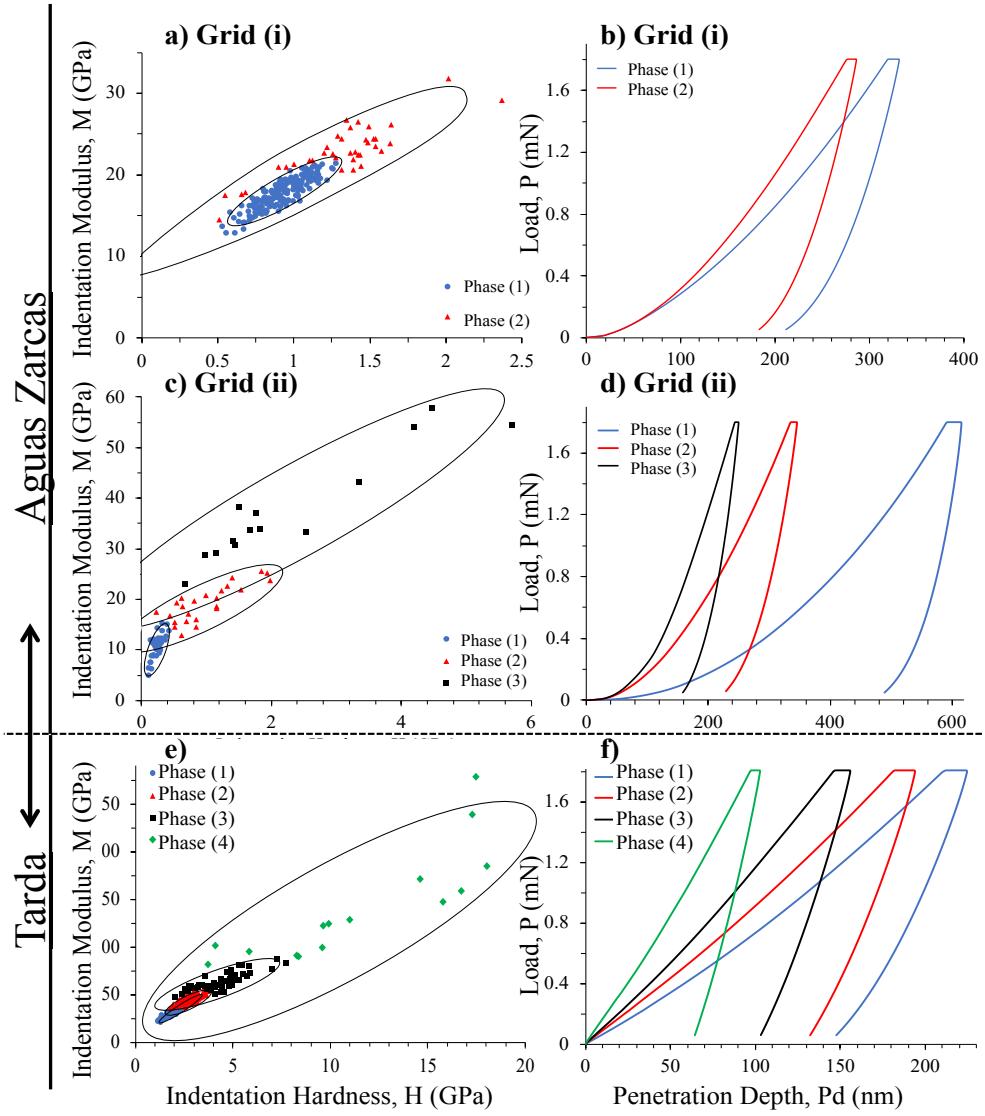

Figure 1. Nano-indentation results on a-d) Aguas Zarcas and e-f) Tarda. a,c&e) Scatter plots of (*M*) vs (*H*) for each point. Each color grouping of data corresponds to a distinct statistical phase. The ellipse major and minor axes are the 95% confidence interval bounds for each phase. a&b) Indentation Grid (i) performed in a serpentine dominated region, and c&d) Grid (ii) includes matrix and chondrules. b,d&f) show the mean load vs. load point displacement curve for each statistical family.

Table 1. Summary of mechanical results from each statistical phase including volume fraction of points belonging to each phase.

		Phase 1		Phase 2		Phase 3		Phase 4		
		mean	std	mean	std	mean	std	mean	std	
	H (GPa)	2.18	0.39	2.74	0.43	4.32	1.28	11.09	4.99	Tarda
	M (GPa)	35.33	5.76	44.31	4.99	61.73	10.46	138.01	57.45	Tarda
	M / H	16.23	1.01	16.3	1.55	14.75	3.13	13.26	4.65	Tarda
	Volume Fraction	0.37		0.45		0.14		0.04		Tarda
Grid (i)	H (GPa)	0.93	0.15	1.21	0.38	NA	NA			Aguas Zarcas
Grid (i)	M (GPa)	17.81	1.85	21.47	3.91	NA	NA			Aguas Zarcas
Grid (i)	M / H	19.44	1.82	18.45	4.23	NA	NA			Aguas Zarcas
Grid (i)	Volume Fraction	0.77		0.23		NA				Aguas Zarcas
Grid (ii)	H (GPa)	0.24	0.07	0.93	0.93	2.33	1.46			Aguas Zarcas
Grid (ii)	M (GPa)	10.72	2.28	18.76	3.76	37.72	10.47			Aguas Zarcas
Grid (ii)	M / H	47.77	11.98	24.14	13.9	35.36	17.36			Aguas Zarcas
Grid (ii)	Volume Fraction	0.47		0.33		0.18				Aguas Zarcas